Cell. Mol. Life Sci. (2013) 70:1255–1268
DOI 10.1007/s00018-012-1200-5

Cellular and Molecular Life Sciences

RESEARCH ARTICLE

Microtubule dynamics alter the interphase nucleus

Gabi Gerlitz · Orly Reiner · Michael Bustin

Received: 31 August 2012 / Revised: 9 October 2012 / Accepted: 15 October 2012 / Published online: 2 November 2012

Abstract Microtubules are known to drive chromosome movements and to induce nuclear envelope breakdown during mitosis and meiosis. Here we show that microtubules can enforce nuclear envelope folding and alter the levels of nuclear envelope-associated heterochromatin during interphase, when the nuclear envelope is intact. Microtubule reassembly, after chemically induced depolymerization led to folding of the nuclear envelope and to a transient accumulation of condensed chromatin at the site nearest the microtubule organizing center (MTOC). This microtubule-dependent chromatin accumulation next to the MTOC is dependent on the composition of the nuclear lamina and the activity of the dynein motor protein. We suggest that forces originating from simultaneous polymerization of microtubule fibers deform the nuclear membrane and the underlying lamina. Whereas dynein motor complexes localized to the nuclear envelope that slide along the microtubules transfer forces and/or signals into the nucleus to induce chromatin reorganization and accumulation at the nuclear membrane folds. Thus, our study identified a molecular mechanism by which mechanical forces generated in the cytoplasm reshape the nuclear envelope, alter the intranuclear organization of chromatin, and affect the architecture of the interphase nucleus.

Keywords Microtubules · Nuclear envelope · Lamins · Chromatin · Dynein

Electronic supplementary material The online version of this article (doi:10.1007/s00018-012-1200-5) contains supplementary material, which is available to authorized users.

G. Gerlitz · M. Bustin
Protein Section, Laboratory of Metabolism,
National Cancer Institute, US National Institutes of Health,
Bethesda, MD 20892, USA

G. Gerlitz · O. Reiner
Department of Molecular Genetics, Weizmann Institute
of Science, 76100 Rehovot, Israel

G. Gerlitz (✉)
Department of Molecular Biology, Ariel University
Center of Samaria, 44837 Ariel, Israel
e-mail: gabi.gerlitz@gmail.com; gabige@ariel.ac.il

Introduction

Microtubules and their interacting proteins play a major role in shaping the architecture of the genome during mitosis and meiosis. At the onset of both mitosis and meiosis, nuclear envelope breakdown is driven by stretching forces generated by the dynein motor proteins that are anchored to it while sliding along microtubules towards the spindle poles [1–3]. Following nuclear envelope breakdown, the microtubules and their motor proteins kinesin and dynein drive the migration of the chromosomes and their attachment to the spindle [4, 5]. Likewise, the generation of the "meiotic bouquet", a cluster of chromosomes that are linked to the nuclear envelope through their telomeres during early stages of meiosis, has been shown to be dependent on microtubules and the associated dynein activity [6]. However, very little is known regarding the ability of the microtubules to sculpture the nuclear morphology and to organize chromatin structures during interphase.

Recent studies have identified a physical link between the microtubules and the nuclear envelope, which facilitates the movement of the nucleus during cellular differentiation and migration [7–12]. This link is based on an interaction between the microtubule motor proteins

kinesin and dynein, and the KASH domain proteins. KASH domain proteins traverse the outer nuclear membrane and protrude into the perinuclear space where they interact with the SUN domain proteins. The SUN domain proteins cross the inner nuclear membrane and interact with nuclear lamins [13, 14], which interact with chromatin both directly [15–18] and indirectly through additional lamina-associated proteins [19, 20]. Thus, the interaction of kinesin and dynein with KASH proteins and the interaction of SUN proteins with the nuclear lamina provide a connection between the cytoplasmic microtubules and the intranuclear chromatin. In lower eukaryotes, a direct association between SUN domain proteins and heterochromatin-associated proteins has been reported [21–24].

The physical link between microtubules and chromatin fibers across the nuclear membrane raises the possibility that microtubules may affect the nuclear shape and the organization of the genome not only during mitosis, but also during interphase when the nuclear envelope is intact. In the study reported here we demonstrated that microtubule recovery from complete disintegration leads to folding of the nuclear envelope and accumulation of condensed chromatin at the site that faces, and is nearest to, the microtubule organizing center (MTOC). The transient accumulation of condensed chromatin at this site is dependent on the composition of the nuclear lamina and on the activity of dynein, which localizes to the nuclear envelope following complete microtubule depolymerization. Our results suggest that forces generated by the microtubule cytoskeleton can reshape both the nuclear membrane and the underlying lamina, and alter the spatial organization of the chromatin fibers during interphase. We demonstrated a mechanism that can facilitate mechanotransduction from the cytoplasm through the nuclear envelope into the nucleus and can induce global changes in chromatin architecture.

Materials and methods

Cell culture and plasmids

Mouse melanoma B16-F1 cells were grown in DMEM (#10564-011; Invitrogen, Grand Island, NY) supplemented with 10 % fetal calf serum (#16000-044; Invitrogen). Microtubule depolymerization was induced by incubation for 3 h in the presence of nocodazole (#M1404; Sigma, Saint Louis, MO) which was added at 5 μg/ml. For microtubule regrowth the cells were washed three times with DMEM to remove the nocodazole and were incubated in growth medium at 37 °C for the indicated periods of time. Cherry fused EB3 was generated by cloning human EB3 into pmCherry-N1. Plasmids expressing histone H1E fused to green fluorescent protein (GFP) (H1E-GFP) [25], lamin A and lamin AΔ50 [26] and $p150^{Glued}$ amino acids 217–548 fused to DsRed ($p150^{217-548}$) [27] were prepared as described in the references. Plasmids were transfected into the cells using Lipofectamine 2000 (#11668-019; Invitrogen, Carlsbad, CA) or jetPEI™ (#101-10; PolyPlus, Illkirch, France).

Immunostaining and live cell imaging

The cells were fixed in 4 % paraformaldehyde in PHEM buffer (60 mM PIPES, pH 6.9, 25 mM HEPES, 10 mM EGTA, 2 mM magnesium acetate) at room temperature for 5 min followed by fixation in methanol supplemented with 1 mM EGTA at −20 °C for another 5 min. Antibodies included mouse monoclonal anti-α-tubulin clone DM1A, 1:400 (#T6199, Sigma, Saint Louis, MO, USA), rabbit polyclonal anti-γ-tubulin, 1:600 (#11321; Abcam, Cambridge, MA), goat polyclonal anti-lamin B, 1:100 (#6216; Santa Cruz Biotechnology, Santa Cruz, CA), and rabbit polyclonal anti-dynein heavy chain, 1:50 (#9115; Santa Cruz Biotechnology). The DNA was stained with Hoechst 33342 (Molecular Probes, Eugene, OR). All images were acquired using a Zeiss LSM META 510 confocal microscope. The ImageJ program was used for quantification of the mean fluorescent signals in the nuclear regions within a circle of radius 5 μm from the MTOC and in the rest of the nucleus. At each point, 11–21 nuclei were analyzed. Statistical significance was calculated using Student's *t* test.

For live cell imaging, the cells were incubated in Leibovit's L15 medium (#21083-027; Invitrogen, Grand Island, NY) supplemented with 10 % fetal calf serum (#16000-044; Invitrogen, Grand Island, NY) in a temperature-controlled chamber. Images were acquired using a DeltaVision system package (Applied Precision, Issaquah, WA). Imaris software (Bitplane, Zurich, Switzerland) was used for movie creation.

Electron microscopy

Samples for electron microscopy were prepared as described previously [28]. Briefly, the cells in six-well plates were fixed with 2 % glutaraldehyde followed by 1 % osmium tetroxide in 0.1 M sodium cacodylate buffer (pH 7.4). Following en bloc staining with 0.5 % uranyl acetate in 0.1 M acetate buffer (pH 5.0), the cells were dehydrated in a series of ethanol dilutions, embedded in epoxy resin, and cured at 55 °C in an oven for 48 h. The hardened resin was separated from the plates by submerging the plates in liquid nitrogen. Thin sections (90 nm) were made parallel to the growth of cells using a diamond knife and an ultramicrotome, mounted on 150 mesh grids, stained in uranyl acetate and lead citrate, and stabilized by carbon

evaporation. The thin sections were examined and imaged with an H7600 Hitachi electron microscope equipped with a CCD camera (AMT, Danvers, MA). In each micrograph the nuclear envelope was divided into two regions: the region that faces the MTOC, which is the region that can be reached by straight lines originating from the MTOC, and the nuclear envelope in the rest of the nucleus. The ImageJ program was used to measure the length of the nuclear envelope in each region as well as the area covered by heterochromatin attached to the nuclear envelope in each region. Nucleoli were distinguished from heterochromatin by the dense fibrillar components that are clearly visualized in transmission electron microscopy (TEM) micrographs. The ratio between the area covered by attached heterochromatin and the length of the nuclear envelope was calculated for each region, and the ratio in the region that faces the MTOC in control cells was set as 1. At each point ten nuclei were analyzed. Statistical significance was calculated using Student's *t* test.

Results

To explore the possibility that microtubules can alter the morphology of the nucleus and the organization of the chromatin fibers during interphase, we induced major and reversible changes in the cellular organization of the microtubules using the microtubule depolymerization agent nocodazole. Following microtubule depolymerization, the nocodazole was washed away to allow microtubule repolymerization. Microtubule repolymerization is initiated at the MTOC, which is localized next to the nucleus and can be visualized by immunofluorescence. We monitored the morphology of the nucleus and the global organization of chromatin by histone H1 fused to GFP and Hoechst staining.

In both control and nocodazole-treated interphase cells, the nuclear envelope appeared smooth and heterochromatin domains seemed randomly spread throughout the nuclei, as visualized by confocal microscopy imaging (Fig. 1a). However, 5 min after removal of nocodazole the nuclear envelope was invaginated at the site closest to and facing the MTOC. In addition, the fluorescent intensities of both H1E-GFP and the Hoechst signal were highly increased at the invagination site, an indication of chromatin accumulation at this site (Fig. 1a, nuclear region is marked with an arrow at the 5-min time point). The extent of the invagination and the accumulation of chromatin next to the MTOC became more prominent 10 min after initiation of microtubule recovery (Fig. 1a, nuclear region is marked with an arrow at the 10-min time point). Interestingly, 30 min after nocodazole removal accumulation of chromatin next to the MTOC and invagination in the nuclear envelope were no longer evident. Thus, microtubule polymerization induced a dynamic reshaping of both the nuclear envelope and the interphase chromatin.

To quantify the degree of chromatin accumulation next to the MTOC, we calculated the mean fluorescent intensities of the H1E-GFP and the Hoechst signals in two different nuclear regions. The first region was the nuclear area nearest to the MTOC (within a circle of radius 5 μm from the MTOC; Fig. 1b, area #1). The second region was the nuclear area more distant from the MTOC (i.e., more than 5 μm away from the MTOC; Fig. 1b, area #2). The ratio of the mean fluorescent signal in area #1 to that in area #2 was defined as the relative signal enrichment next to the MTOC. This showed that 10 min after initiation of microtubule recovery, the chromatin concentration at the invagination site facing the MTOC increased by 50 %, as compared to the chromatin concentration in the regions that were more distant from the MTOC. In sharp contrast, in control cells and in cells 30 min after nocodazole removal no relative signal enrichment next to the MTOC was observed. These results indicate that microtubule repolymerization induces significant transient changes in the shape of the nucleus and in the spatial organization of the intranuclear chromatin.

To monitor the kinetics of these nuclear changes in live cells we labeled the chromatin and the MTOC by overexpressing H1E-GFP and EB3-Cherry, respectively. Chromatin accumulation at the invaginated nuclear envelope site facing the MTOC was first clearly noticeable in frame 05:54. The intensity was most prominent 2 min later, in frame 07:53. Chromatin dispersal from that site was first observable in frame 19:45, i.e., around 20 min after initiation of microtubule repolymerization (Fig. 2, and Supplementary material). Thus, the entire process from the initiation of chromatin accumulation at the invagination site to its dispersal from that site lasted only 15–17 min.

To obtain additional insight into the dynamic changes occurring in the nuclear envelope during microtubule recovery from nocodazole treatment we immunostained the cells with antibodies to lamin B. The kinetics of lamin B accumulation next to the MTOC were very similar to the kinetics of chromatin accumulation (Fig. 3). Within 5 min of microtubule recovery, lamin B accumulated at the invaginated nuclear membrane next to the MTOC. The signal was more prominent 10 min after initiation of recovery, but was no longer visible at 30 min. Lamin B is known to be stably incorporated into the mesh of the nuclear lamina. Live cell imaging analysis has revealed that once incorporated, lamin B does not diffuse out of the nuclear lamina [26, 29]. Therefore, the transient accumulation of lamin B at the nuclear membrane invagination site most likely indicates accumulation of nuclear envelope mesh, rather than accumulation of free lamin B proteins in this region.

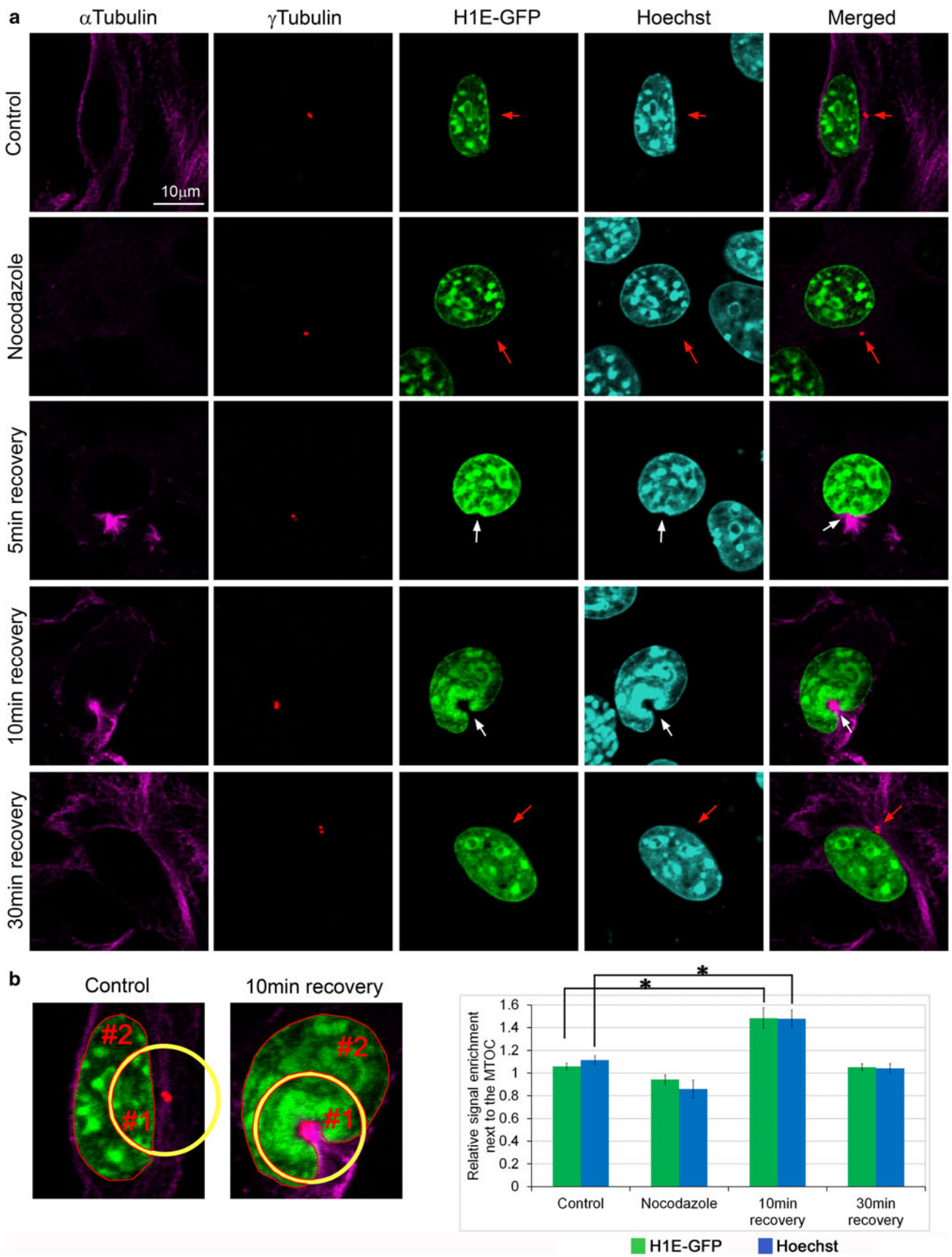
a
αTubulin
γTubulin
H1E-GFP
Hoechst
Merged
Control
Nocodazole
5min recovery
10min recovery
30min recovery
10μm
b
Control
10min recovery
#2
#1
Relative signal enrichment next to the MTOC
1.6
1.4
1.2
1
0.8
0.6
0.4
0.2
0
*
*
Control
Nocodazole
10min recovery
30min recovery
H1E-GFP
Hoechst

◀ **Fig. 1** Microtubule recovery induces nuclear alterations. **a** Microtubule depolymerization was induced by nocodazole treatment in cells expressing histone H1E-GFP. Following nocodazole removal the cells were further incubated for the indicated times to allow microtubule polymerization. Following fixation, the cells were stained with antibodies to α-tubulin to visualize microtubules, γ-tubulin to visualize the MTOC, and with Hoechst reagent to visualize the DNA. The *Merged* images show the merged signals of α-tubulin, γ-tubulin and H1E-GFP (*white arrows* accumulated chromatin next to the MTOC; *red arrows* MTOC in control cells, nocodazole-treated cells and in cells 30 min after nocodazole removal, in which no chromatin accumulated next to the MTOC; *scale bar* 10 μm). **b** Quantification of the kinetics of the changes in signal intensities of H1E-GFP and Hoechst staining in the nuclear region next to the MTOC. For quantification, circles with a radius of 5 μm were centered at the MTOC as shown in the magnified images (*yellow circles*). The nuclear regions inside the circles (*area #1*) and outside the circle (*area #2*) were selected (marked with *red lines*) using the ImageJ program and the mean fluorescent signals of the green channel and blue channel in each region were measured (*green bars*, *blue bars*). The relative signal enrichment next to the MTOC was determined as the ratio of the mean fluorescent signal of area #1 to the mean fluorescent signal of area #2, and the average (±SE) relative signal enrichment values for each time point are shown in the bar graph. $*P < 0.001$, Student's *t* test

The structural changes occurring in the nucleus were even more obvious when examined at high resolution by TEM. Thus, in cells 10 min after nocodazole removal, TEM analysis revealed intensive folding and invagination of the nuclear envelope only in the nuclear region facing the MTOC (Fig. 4a). Significantly, in regions that did not face the MTOC and in control cells that were not exposed to nocodazole the nuclear envelope remained unfolded and free of significant invaginations. Likewise, TEM analysis revealed significant localization of condensed chromatin at the invagination sites facing the MTOC in nocodazole-treated cells, but not in nontreated control cells.

To quantify the relative levels of accumulation of condensed chromatin at the folded nuclear envelope, we distinguished between two regions of the nuclear envelope. The first region contained the nuclear envelope segments that could be reached by straight lines originating from the MTOC; this region was called "the nuclear envelope next to the MTOC" (Fig. 4a, red lines). The second region contained all nuclear envelope segments that were not included in the first region and was called "the rest of the nucleus". The lengths of the nuclear envelope segments in both parts of the nucleus were measured. Next, we measured separately the areas of condensed chromatin (heterochromatin) in contact with each of the above nuclear envelope segments. The ratio of the heterochromatin area to the nuclear envelope length in each region is a measure of the relative levels of nuclear envelope-associated heterochromatin. This ratio was set as 1 for the MTOC-facing region in control cells (Fig. 4b). These measurements indicate that per unit of nuclear envelope length, the amount of heterochromatin associated with the folded nuclear envelope was 80 % higher than that in the unfolded region of the nuclear envelope (Fig. 4b). Thus, the TEM results are in full agreement with the results of confocal microscope imaging of fixed cells (Fig. 1) and with those of fluorescent microscope imaging of live cells (Fig. 2, and Supplementary material), indicating that during microtubule repolymerization heterochromatin accumulates at the nuclear envelope folds facing the MTOC. Taken together, these results suggest that microtubule polymerization can lead to dynamic changes in the structure of the nucleus: both the nuclear envelope and the spatial organization of the chromatin fibers were reversibly altered. Thus, structural changes occurring in the cytoplasm dynamically reshape the nucleus.

The nuclear lamina plays a major role in determining the mechanical properties of the nuclear envelope and is also in direct physical contact with chromatin [12, 30, 31]. Therefore, we tested whether the composition of the nuclear lamina may play a role in the transient accumulation of chromatin at the nuclear envelope folds. For this purpose, we followed the accumulation of chromatin during microtubule repolymerization in cells overexpressing lamin A or lamin AΔ50 fused to GFP (Fig. 5a). Lamin AΔ50 is a truncated form of lamin A that lacks the 50 C-terminal amino acids, which is the Hutchinson-Gilford progeria syndrome mutated lamin A [32, 33]. The lamin AΔ50 map of protein–protein interaction only partially overlaps that of lamin A [17]. It is also thought that nuclear envelope containing lamin AΔ50 has altered mechanical properties in comparison to nuclear envelope containing lamin A [26, 34]. We found that expression of GFP-fused lamin AΔ50 did not interfere with microtubule-driven chromatin accumulation. In contrast, overexpression of GFP-fused lamin A almost completely inhibited microtubule-driven chromatin accumulation (Fig. 5).

The mean fluorescent signal of the Hoechst reagent was measured in two nuclear regions and quantified as described in Fig. 1 (Fig. 5b). Thus, the first region was the nuclear area within a circle of radius 5 μm from the MTOC and the second region was the nuclear area that was more than 5 μm distant from the MTOC. The ratio of the Hoechst mean fluorescent signal in the first nuclear region to that in the second nuclear region is an indication of the relative signal enrichment next to the MTOC. In control and in GFP-fused lamin AΔ50-expressing cells 10 min after induction of microtubule recovery, the chromatin concentration next to the MTOC was more than 1.6-fold higher than in more distant parts of the nucleus. However, in cells overexpressing GFP-fused lamin A the chromatin concentration next to the MTOC was only 1.2-fold higher than in more distant parts of the nucleus. Thus overexpression of lamin A inhibited the accumulation of

chromatin next to the MTOC by more than 60 %. Accumulation of chromatin next to the MTOC in these cells was not observed at additional time points (not shown), indicating that lamin A overexpression inhibited rather than changed the kinetics of the microtubule-driven nuclear alterations. Interestingly, lamin A overexpression interfered with microtubule-driven chromatin accumulation next to the MTOC, but not with nuclear envelope folding. In most cases, nuclear envelope invaginations were observed while chromatin failed to accumulate next to the MTOC. These results suggest that the concentration of lamin A in the nuclear envelope is critical for establishing a link between the nuclear envelope and the chromatin fibers.

Rupture of the nuclear envelope during mitosis is microtubule-driven and is thought to be dependent on the activity of the plus-end-directed motor protein complex, dynein [2]. Indeed we found that nocodazole treatment led to accumulation of dynein on the nuclear envelope (Fig. 6), a finding fully consistent with previous observations [35, 36]. Therefore, we examined whether dynein activity is important for microtubule-driven chromatin accumulation. Dynein activity is dependent on the dynactin protein complex, which is important for targeting dynein to specific cellular locations, for linking dynein to its cargos, and for increasing dynein processivity [37, 38]. Expression of the dynein binding fragment of the dynactin subunit, $p150^{Glued}$ ($p150^{217–548}$) has been shown to inhibit dynein activity [27]. Therefore, the effect of microtubule recovery from nocodazole treatment on chromatin organization was evaluated in cells expressing the dynein inhibitor $p150^{217–548}$ (Fig. 7). Interestingly, expression of $p150^{217–548}$ inhibited the accumulation of chromatin next to the MTOC during microtubule recovery from nocodazole treatment, as evaluated by Hoechst staining. For quantification, the Hoechst signals in the nuclear region next to the MTOC (within a circle of radius 5 μm from the MTOC) and in the rest of the

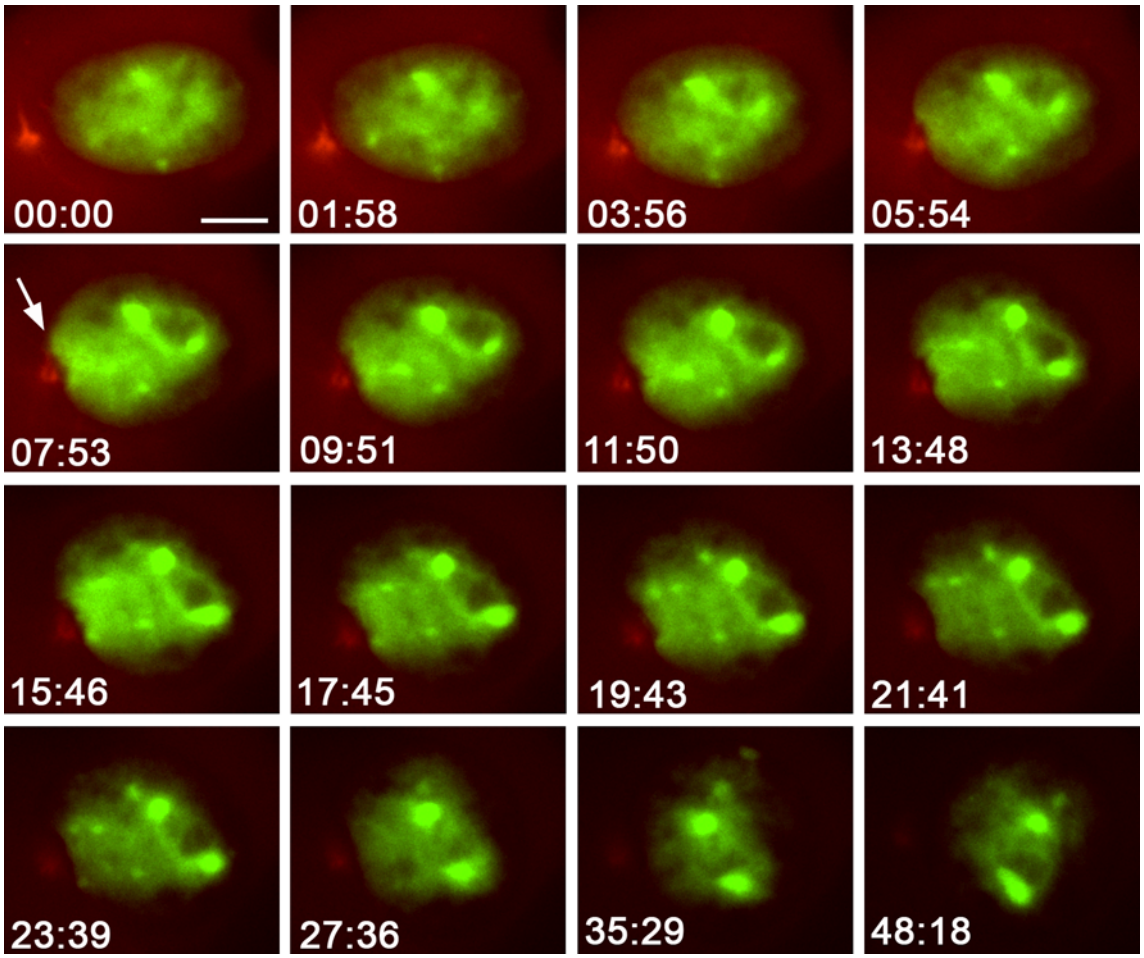

Fig. 2 Microtubule recovery induces nuclear alterations. Shown are time-lapse images. Cells overexpressing both H1E-GFP (chromatin marker) and Cherry fused EB3 (MTOC marker) were treated with nocodazole to induce microtubule depolymerization. After nocodazole removal, the cells were imaged every minute for 50 min; 2 min elapsed between nocodazole removal and acquisition of the first frame, therefore 2 min should be added to the acquisition time shown in each image. Selected images are presented (*image 07:53* first frame in which significant chromatin accumulation next to the MTOC (*arrow*) can be seen; *scale bar* 8 μm)

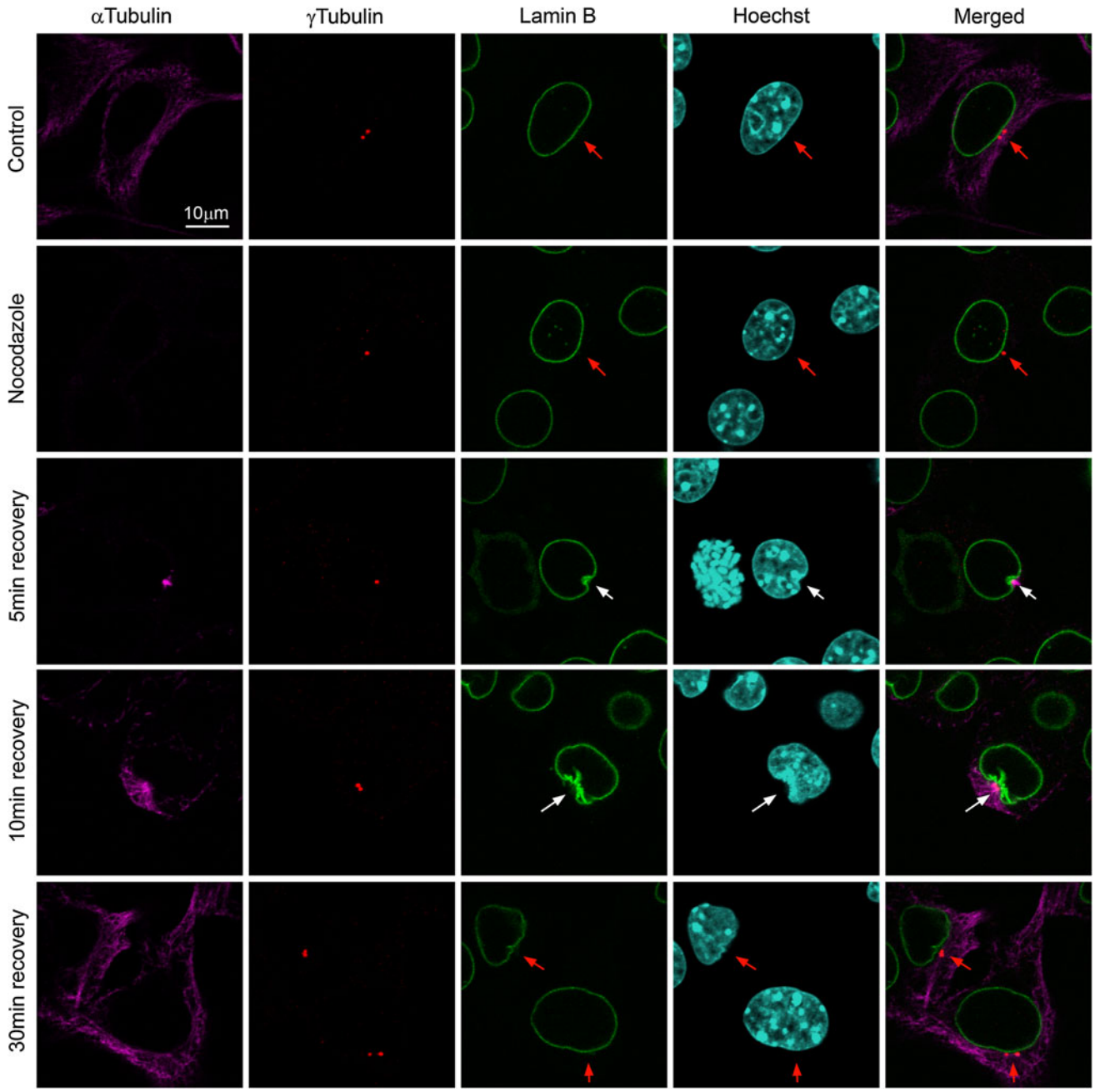

Fig. 3 Microtubule recovery induces reshaping of the nuclear envelope. Microtubule depolymerization was induced by nocodazole treatment. After nocodazole removal the cells were further incubated for the indicated times to allow microtubule polymerization. After fixation, the cells were stained with antibodies to α-tubulin to visualize the microtubules, γ-tubulin to visualize the MTOC, lamin B to visualize the nuclear envelope, and with Hoechst reagent to visualize the DNA. The *Merged* images show the merged signals of α-tubulin, γ-tubulin and lamin B (*white arrows* accumulated lamin B and chromatin next to the MTOC; *red arrows* MTOC in control cells, nocodazole-treated cells and cells 30 min after nocodazole removal, in which no lamin B or chromatin accumulated next to the MTOC; *scale bar* 10 μm)

nucleus were compared, as shown in Fig. 1. This analysis revealed that in control cells 10 min after initiation of microtubule recovery the chromatin concentration close to the MTOC was 50 % higher than in regions distant from the MTOC (Fig. 7b). However, in cells expressing the dynein inhibitor $p150^{217–548}$ 10 min after initiation of microtubule recovery there was an increase of only 19 % in the chromatin concentration close to the MTOC in comparison to more distant nuclear regions. Interestingly, inhibition of dynein activity interfered only with microtubule-driven chromatin accumulation next to the MTOC, while nuclear envelope folding was not affected and still occurred. These

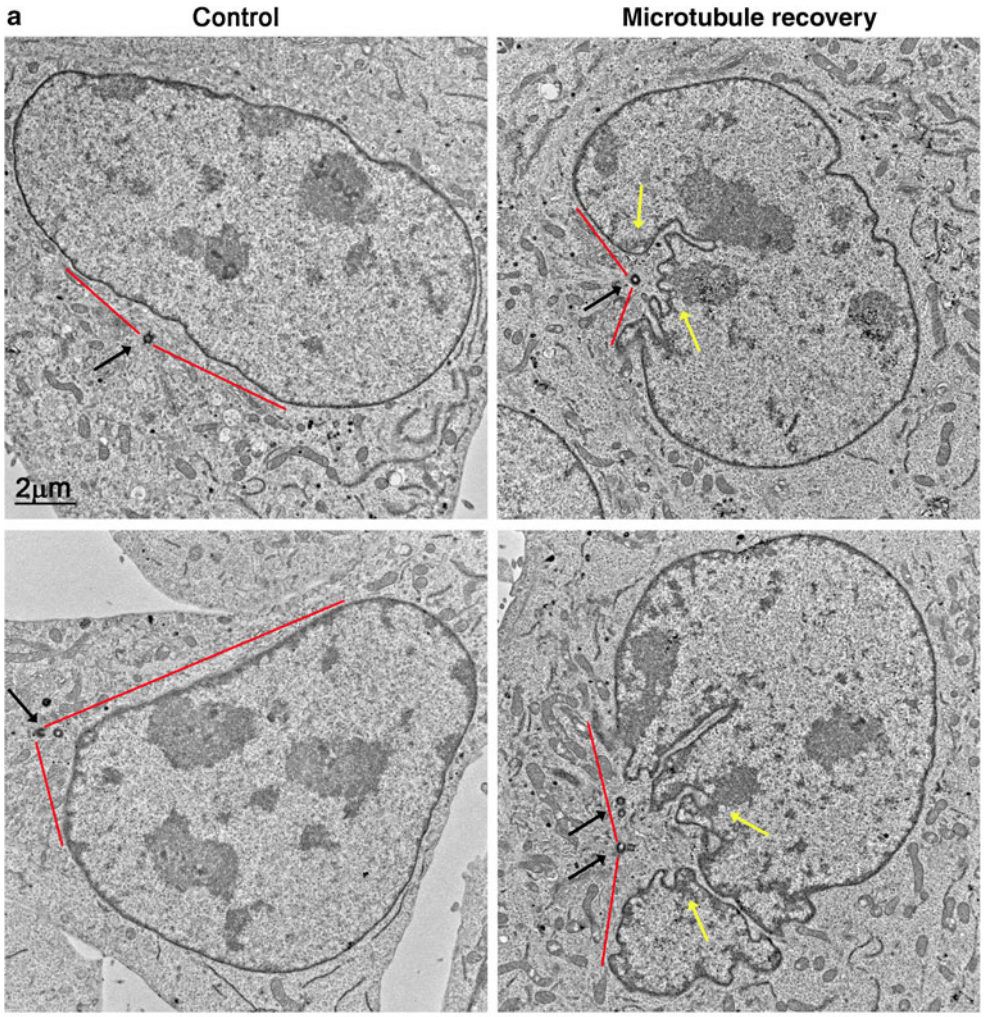

results suggest that the function of the dynein complexes linked to the nuclear envelope, which are formed during the nocodazole treatment, is important for microtubule-driven reorganization of chromatin.

Discussion

In the study reported here we showed that microtubule polymerization, a cytoplasmic process, reshapes the

◀ **Fig. 4** Microtubule recovery induces nuclear envelope folding and an increase in heterochromatin association with the nuclear envelope in the nuclear region that faces the MTOC. **a** TEM images of control cells and cells after 10 min of microtubule reassembly (*black arrows* centrosomes, *red lines* nuclear envelope parts that face the MTOC, *yellow arrows* heterochromatin patches linked to the nuclear envelope, *scale bar* 2 μm). **b** Quantification of the relative amounts of heterochromatin associated with the nuclear envelope. The nuclear envelope was divided into two regions. The first region contained the nuclear envelope segments that could be reached by straight lines originating from the MTOC (**a** *red lines*) and was called "the nuclear envelope next to the MTOC". The second region contained all nuclear envelope segments that were not included in the first region and was called "the rest of the nucleus". The areas of heterochromatin in contact with each of the above nuclear envelope segments were measured separately. The ratio of the area of heterochromatin linked to the nuclear envelope of each region to the nuclear envelope length in each region is a measure of the relative level of nuclear envelope-associated heterochromatin. This ratio for the MTOC facing region in control cells was set as 1. The bar graph represents the mean (±SE) relative levels of nuclear envelope-associated heterochromatin in ten different cells. $*P < 0.005$, Student's t test

nuclear envelope and the chromatin fibers inside the interphase nucleus. The microtubule-driven alterations in the nuclear envelope and the accumulation of heterochromatin at the invagination site of the nuclear envelope are highly dynamic and reversible processes (Figs. 1, 2, 3, 4). During microtubule recovery from nocodazole treatment there is a time window of 15–20 min in which the microtubules induce nuclear envelope folding and accumulation of condensed chromatin at the nuclear site that is the closest to the MTOC. The ability of the microtubules to reshape the nuclear architecture is dependent on the levels of lamin A (Fig. 5) and on the function of the microtubule motor protein, dynein (Fig. 7).

Our knowledge of the ability of microtubules to reshape the nucleus during interphase is very limited. In *Drosophila* embryonic development, during cellularization all cortical nuclei are enclosed by membranes while the nuclei change from spherical to ellipsoid. During this process, which is dependent on both microtubule polymerization and the nuclear lamina protein Kugelkern, accumulation of heterochromatin also occurs at the side of the nucleus closest to the MTOC [39, 40]. An additional example of microtubule-driven nuclear reshaping is nuclear lobulation during granulocytic differentiation. During the 2 weeks of granulocytic differentiation, lobulation of the nucleus is associated with intensive nuclear envelope folding and chromatin condensation [41, 42]. In vitro granulocytic differentiation of HL60 cells is dependent on microtubule dynamics, since nocodazole treatment inhibits it [43]. Interestingly, this differentiation process is also associated with a reduction in lamin A levels [43, 44] and a decrease in the phosphorylation level of histone H1 [45]. The similarity between the characteristics of granulocytic differentiation and our observations on the effects occurring during microtubule recovery from nocodazole treatment suggests that these processes may be mechanistically similar.

We envision two possible processes that can account for the effects of microtubule recovery on the morphology of the nuclear envelope: first, the simultaneous encounter of the newly formed microtubule fibers with the nuclear envelope generates sufficient force to push the nuclear envelope inwards, and second, dynein motor complexes, which are anchored to the nuclear envelope due to the nocodazole treatment (Fig. 6) [35, 36], attach to the newly polymerized microtubule fibers once the nocodazole is removed. Sliding of these dynein complexes along the microtubules towards the MTOC pulls the nuclear envelope towards the MTOC around the polymerized microtubules, thereby leading to the folding of the nuclear envelope. Our observation that dynein does not inhibit nuclear envelope folding during microtubule recovery (Fig. 7a) suggests that nuclear folding is dynein-independent. Thus, it is more probable that nuclear envelope folding is generated by microtubule fibers that simultaneously encounter the nuclear envelope (Fig. 7c). In this scenario, after nocodazole removal, synchronization of microtubule dynamics gradually decreases. Thus, with time fewer microtubule fibers encounter the nuclear envelope simultaneously at each folded point, the forces that led to nuclear envelope folding are decreased and the recovery of the nuclear envelope from the folded morphology to its "regular" spherical morphology is enabled.

By itself, folding of the nuclear envelope is not sufficient to condense trapped chromatin between the nuclear envelope invaginations, since both overexpression of lamin A (Fig. 5) and inhibition of dynein activity (Fig. 7a, b) interfered with the accumulation of condensed chromatin next to the MTOC without disrupting nuclear envelope invagination and folding. Thus, accumulation of condensed chromatin is dependent on both the lamina composition and the activity of the dynein motor complex. An increase in lamin A levels could affect microtubule-driven chromatin accumulation either by elevating the rigidity of the nuclear envelope or by interfering with the formation of protein–protein interactions, which are necessary for the connection between the microtubules and chromatin. The former option seems less probable for two reasons. First, previous studies have indicated that Hutchinson-Gilford progeria syndrome cells expressing the lamin AΔ50 mutant have a more rigid nuclear envelope than wild-type cells [26, 34]. Therefore, it would be expected that the nuclear envelope in lamin AΔ50-overexpressing cells is more rigid than in lamin A-overexpressing cells, yet only overexpression of lamin A inhibited the microtubule-driven chromatin accumulation. Second, overexpression of lamin A did not interfere with microtubule-driven nuclear envelope folding, suggesting that no increase in nuclear

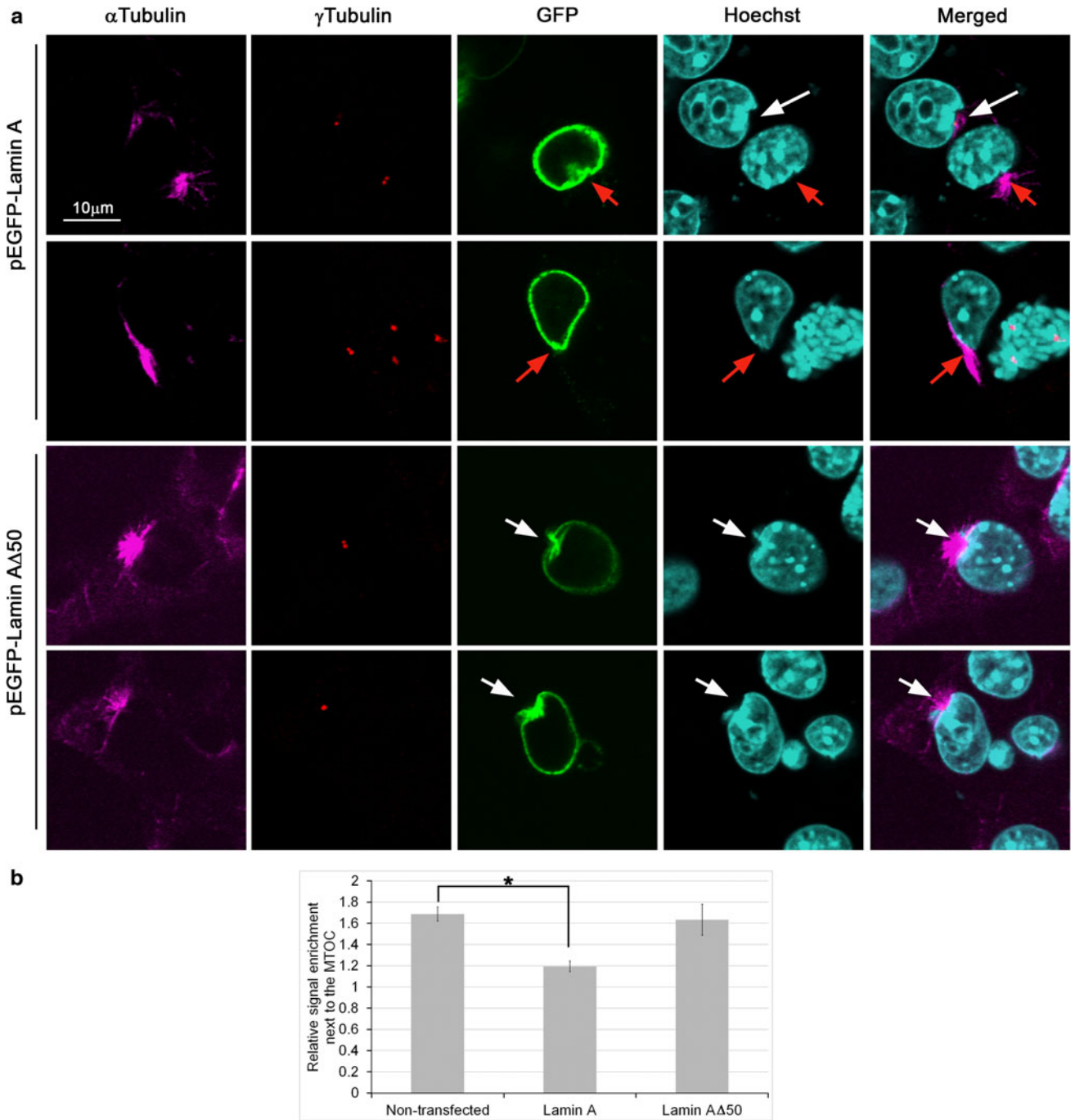

Fig. 5 Chromatin reorganization during microtubule recovery is dependent on the composition of the nuclear lamina. **a** Nocodazole-mediated microtubule depolymerization was induced in cells overexpressing GFP-fused lamin A or lamin AΔ50. After nocodazole removal, the cells were incubated for a further 10 min to allow microtubule polymerization, fixed and stained with antibodies to α-tubulin and γ-tubulin. DNA was stained with Hoechst reagent. The *Merged* images show the merged signals of α-tubulin, γ-tubulin and GFP fused lamins (*white arrows* accumulated chromatin next to the MTOC in GFP-fused lamin AΔ50-expressing cells and in a nontransfected cells, *red arrows* MTOC in cells overexpressing GFP-fused lamin A, *scale bar* 10 μm). **b** Quantification of the relative amount of chromatin in the nuclear region next to the MTOC in the different cells 10 min after nocodazole removal. The mean fluorescent signals of the Hoechst reagent in the nuclear regions within a circle of radius 5 μm from the MTOC were normalized to the mean (±SE) fluorescent signals in the rest of the nucleus. $^*P < 0.001$, Student's *t* test

envelope rigidity occurred in these cells. We therefore favor the possibility that overexpression of lamin A disrupts protein–protein interactions that are important for maintaining a proper link between the nuclear envelope and chromatin. In this respect we note that a recent study identified 35 proteins which interact preferentially with

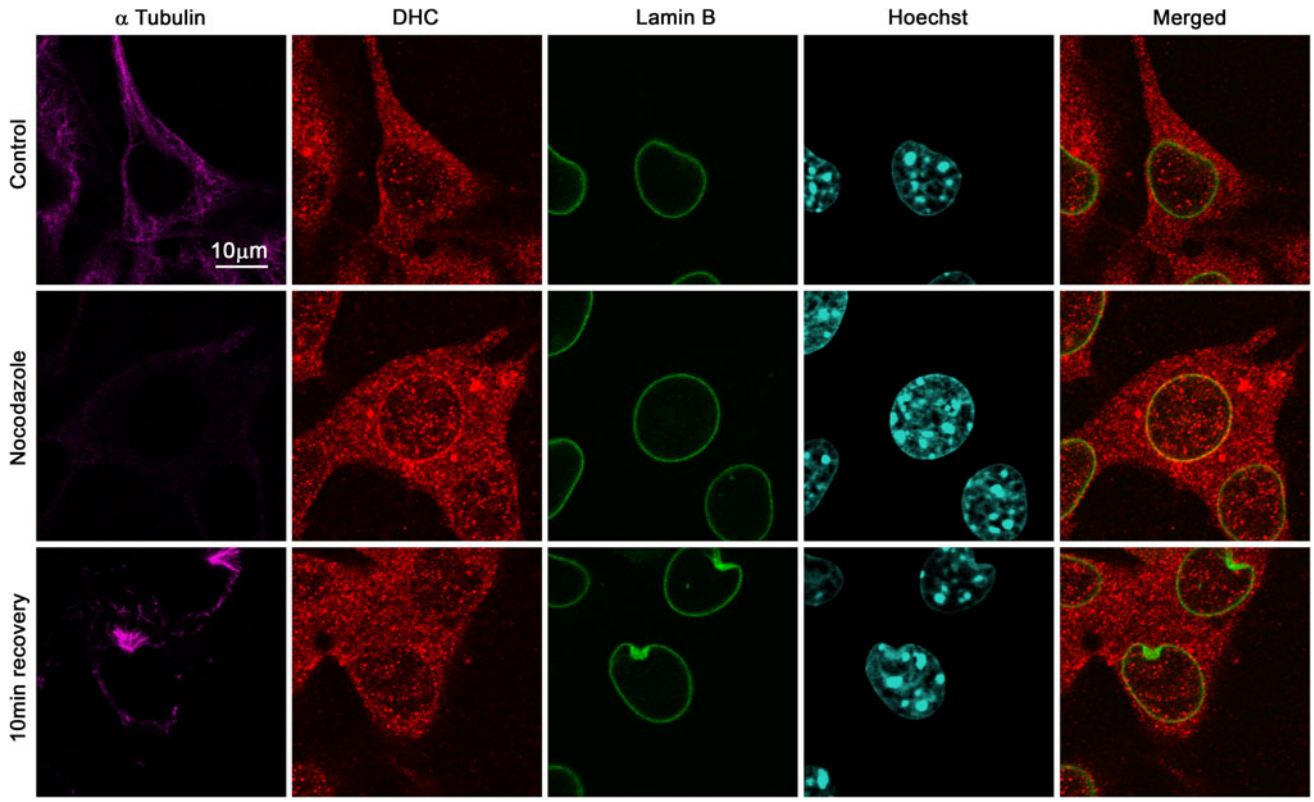

Fig. 6 Nocodazole treatment induces dynein accumulation on the nuclear envelope. Microtubule depolymerization was induced by nocodazole treatment. After nocodazole removal the cells were incubated for a further 10 min to allow microtubule polymerization. At the indicated times, the cells were fixed and stained with antibodies to α-tubulin, dynein heavy chain (*DHC*), lamin B and Hoechst reagent. The *Merged* images show the signals of dynein heavy chain and lamin B (*scale bar* 10 μm)

lamin A over lamin AΔ50 [17]. Therefore, it is probable that overexpression of lamin A rather than lamin AΔ50 would have a dominant negative effect due to interference with protein–protein interactions that are important for the link between the nuclear envelope and the chromatin fibers or that between the nuclear envelope and the microtubules.

Inhibition of dynein activity led to interference with microtubule-driven accumulation of condensed chromatin next to the MTOC. Dynein motor complexes, which are anchored to the nuclear envelope by nocodazole treatment (Fig. 6) [35, 36] can form a link between the emerging microtubule fibers and chromatin. Components of the dynein complex have been shown to interact with KASH domain proteins that traverse the outer nuclear membrane [7, 11]. KASH domain proteins are able to bind SUN domain proteins that traverse the inner nuclear membrane into the nucleus [13, 14], where they are able to bind lamins [46–48]. Lamins are known to associate with chromatin [15–20]. Thus, a physical link between the forming microtubule fibers and chromatin may be formed upon initiation of microtubule recovery from nocodazole treatment. We hypothesize that establishment of this link generates tension at the nuclear lamina, which may alter interactions of the lamins with their protein partners, thereby leading to better interaction of lamins with heterochromatin-associated proteins, thus resulting in accumulation of heterochromatin in the nuclear envelope region facing the MTOC (Fig. 7c). As the microtubule fibers recover from nocodazole treatment, the dynein motor complexes dissociate from the nuclear envelope, thereby stopping the transmission of forces to the nuclear lamina resulting in the dispersal of the condensed chromatin from the nuclear envelope.

Attempts to further characterize the condensed chromatin accumulated next to the MTOC by immunostaining it with antibodies to various chromatin components such as histone H1, HMGN1 or several histone modifications were not successful, suggesting that the antibodies could not efficiently bind to their cognate sites in this condensed chromatin.

Based on all our observations, we suggest the following model for the mechanism by which the microtubule cytoskeleton alters both nuclear morphology and chromatin organization (Fig. 7c). Following nocodazole removal, the coordinated assembly of new microtubule fibers generates sufficient mechanical force to invaginate and fold the nuclear envelope. Concurrently, dynein motor complexes, which are anchored to the nuclear envelope by nocodazole

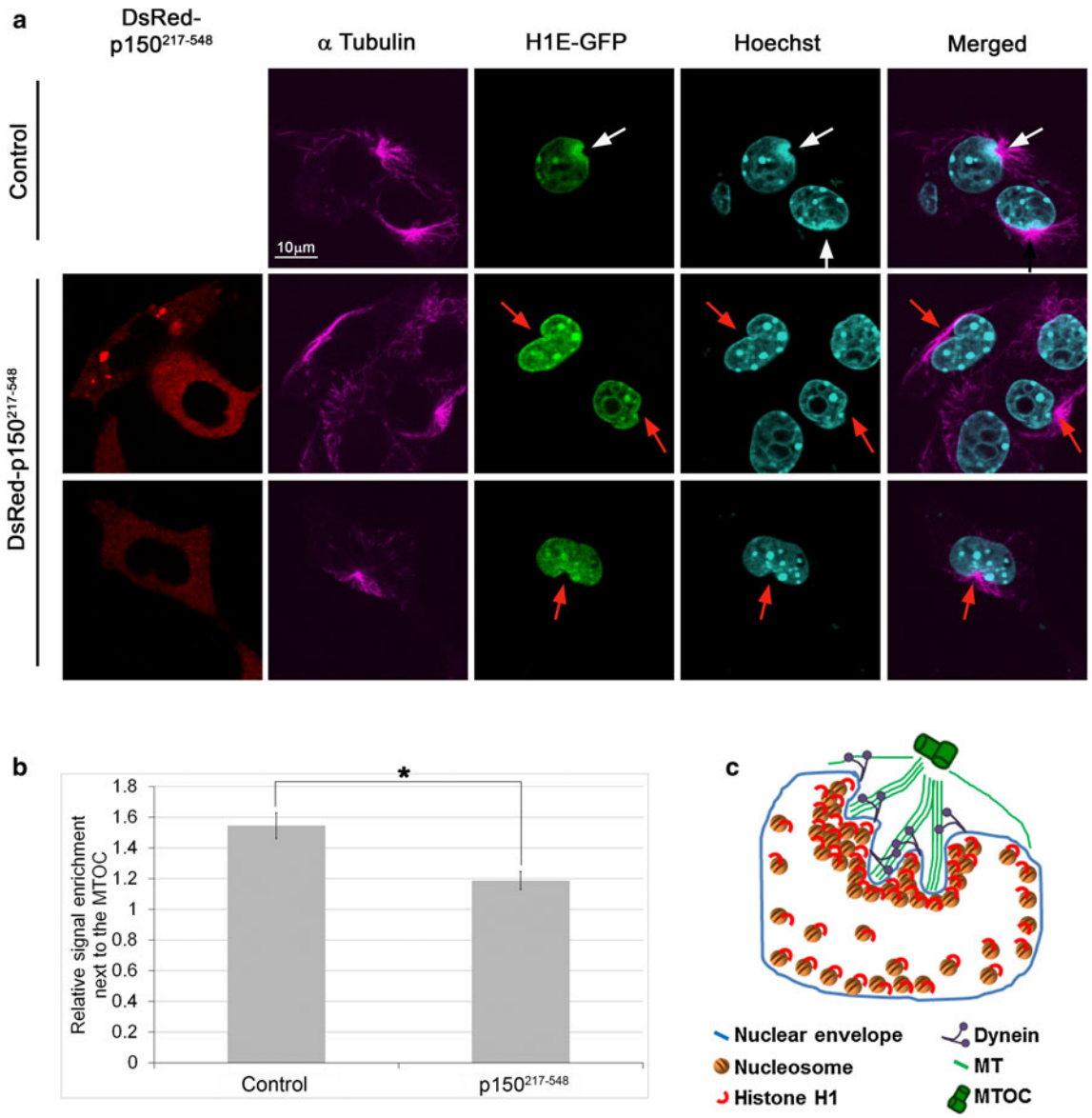

Fig. 7 Chromatin reorganization during microtubule recovery is dependent on the function of dynein. **a** Microtubule depolymerization was induced by nocodazole treatment in cells expressing both H1E-GFP and the dynein inhibitor, $p150^{217–548}$ fused to DsRed, and in control cells expressing only H1E-GFP. After nocodazole removal the cells were incubated for a further 10 min to allow microtubule polymerization, fixed and stained with antibodies to α-tubulin and Hoechst reagent. The *Merged* images show the signals of α-tubulin and Hoechst reagent (*white arrows* accumulated chromatin next to the MTOC in control cells, *red arrows* MTOC in cells expressing $p150^{217–548}$, *scale bar* 10 μm). **b** Quantification of the relative amounts of chromatin in the nuclear region next to the MTOC in control cells and in cells expressing the dynein inhibitor, $p150^{217–548}$ fused to DsRed 10 min after nocodazole removal. The mean fluorescent signals of the Hoechst reagent in the nuclear regions within a circle of radius 5 μm from the MTOC were normalized to the mean (±SE) fluorescent signals in the rest of the nucleus. $*P < 0.003$, Student's *t* test. **c** Diagram of microtubule-driven nuclear reorganization. After nocodazole removal, the coordinated assembly of new microtubule fibers generates sufficient mechanical force to invaginate and fold the nuclear envelope. Concurrently, dynein motor complexes, which are anchored to the nuclear envelope due to the nocodazole treatment, attach to the newly polymerized microtubule fibers, thereby forming a physical bridge between the cytoplasmic microtubule cytoskeleton and the chromatin fibers inside the nucleus. Sliding of these dynein complexes along the microtubules towards the MTOC generates strain at the nuclear lamina, altering the interaction of the lamins with nuclear proteins, thereby enhancing the interaction of the lamins with heterochromatin-associated proteins, thus leading to the accumulation of heterochromatin at the nuclear envelope region facing the MTOC

treatment, attach to the newly polymerized microtubule fibers, thereby forming a physical bridge between the cytoplasmic microtubule cytoskeleton and the chromatin fibers inside the nucleus. Sliding of these dynein complexes along the microtubules towards the MTOC generates strain at the nuclear lamina, altering the interaction of the lamins

with nuclear proteins, thereby enhancing the interactions of lamins with heterochromatin-associated proteins, thus leading to the accumulation of heterochromatin in the nuclear envelope region facing the MTOC.

According to this model, induction of dynein interaction with the nuclear envelope can lead to heterochromatin accumulation in the nuclear envelope region that faces the MTOC. Interestingly, accumulation of dynein on the nuclear envelope has been shown in migrating neurons, where dynein motor proteins pull the nucleus forward [7, 13]. Furthermore, reexamination of classical TEM micrographs of migrating neurons has revealed accumulation of heterochromatin at the side of the nucleus facing the MTOC [49]. In addition, nuclear migration in the filamentous fungi *Neurospora crassa* is associated with accumulation of heterochromatin at the leading tip of the motile nuclei, where dynein is predicted to pull the nucleus towards the MTOC [25, 50]. Thus, microtubule-driven nuclear alterations may be highly important during cell migration.

In addition, our data support the view that the entire cell functions as a tensionally integrated (tensegrity) system. In such a system components that are physically connected to each other balance forces generated by various components in the system to stabilize the entire structure of the system [51, 52]. Our results suggest that pulling forces generated by the microtubule network lead to chromatin condensation next to the nuclear envelope to oppose these forces. This mechanism may also be used for mechanotransduction from the cytoplasm into the nucleus: changes in the cytoplasmic cytoskeleton are transmitted mechanically to alter the nuclear architecture leading to changes in chromatin function.

Acknowledgments We thank Trina A. Schroer (Department of Biology, Johns Hopkins University, Baltimore, MD, USA), Michael W. Davidson (National High Magnetic Field Laboratory and Department of Biological Science, Florida State University, Tallahassee, FL, USA) and Tom Misteli (NCI, NIH, MD, USA) for providing the plasmids, Valarie A. Barr (LCMB, NCI, NIH) for help with the confocal microscopy, and Kunio Nagashima and Christina M. Burks (Electron Microscope Laboratory, Advanced Technology Program, SAIC-Frederick, Inc. NCI, NIH, Frederick, MD, USA) for help with the TEM analysis. This work was supported by the Intramural Research Program of the National Institutes of Health, Center for Cancer Research, National Cancer Institute.

References

1. Salina D, Bodoor K, Eckley DM, Schroer TA, Rattner JB, Burke B (2002) Cytoplasmic dynein as a facilitator of nuclear envelope breakdown. Cell 108(1):97–107. pii:S0092867401006286
2. Beaudouin J, Gerlich D, Daigle N, Eils R, Ellenberg J (2002) Nuclear envelope breakdown proceeds by microtubule-induced tearing of the lamina. Cell 108(1):83–96. pii:S0092867401006274
3. Burke B, Ellenberg J (2002) Remodelling the walls of the nucleus. Nat Rev Mol Cell Biol 3(7):487–497. doi:10.1038/nrm860
4. Gatlin JC, Bloom K (2010) Microtubule motors in eukaryotic spindle assembly and maintenance. Semin Cell Dev Biol 21(3):248–254. doi:10.1016/j.semcdb.2010.01.015
5. Walczak CE, Cai S, Khodjakov A (2010) Mechanisms of chromosome behaviour during mitosis. Nat Rev Mol Cell Biol 11(2):91–102. doi:10.1038/nrm2832
6. Hiraoka Y, Dernburg AF (2009) The SUN rises on meiotic chromosome dynamics. Dev Cell 17(5):598–605. doi:10.1016/j.devcel.2009.10.014
7. Zhang X, Lei K, Yuan X, Wu X, Zhuang Y, Xu T, Xu R, Han M (2009) SUN1/2 and Syne/Nesprin-1/2 complexes connect centrosome to the nucleus during neurogenesis and neuronal migration in mice. Neuron 64(2):173–187. doi:10.1016/j.neuron.2009.08.018
8. Malone CJ, Misner L, Le Bot N, Tsai MC, Campbell JM, Ahringer J, White JG (2003) The *C. elegans* hook protein, ZYG-12, mediates the essential attachment between the centrosome and nucleus. Cell 115(7):825–836. S0092867403009851 [pii]
9. Fischer JA, Acosta S, Kenny A, Cater C, Robinson C, Hook J (2004) Drosophila klarsicht has distinct subcellular localization domains for nuclear envelope and microtubule localization in the eye. Genetics 168(3):1385–1393. doi:10.1534/genetics.104.028662
10. Roux KJ, Crisp ML, Liu Q, Kim D, Kozlov S, Stewart CL, Burke B (2009) Nesprin 4 is an outer nuclear membrane protein that can induce kinesin-mediated cell polarization. Proc Natl Acad Sci USA 106(7):2194–2199. doi:10.1073/pnas.0808602106
11. Fridolfsson HN, Ly N, Meyerzon M, Starr DA (2010) UNC-83 coordinates kinesin-1 and dynein activities at the nuclear envelope during nuclear migration. Dev Biol 338(2):237–250. doi:10.1016/j.ydbio.2009.12.004
12. Wilson KL, Berk JM (2010) The nuclear envelope at a glance. J Cell Sci 123(Pt 12):1973–1978. doi:10.1242/jcs.019042
13. Starr DA, Fridolfsson HN (2010) Interactions between nuclei and the cytoskeleton are mediated by SUN-KASH nuclear-envelope bridges. Annu Rev Cell Dev Biol 26:421–444. doi:10.1146/annurev-cellbio-100109-104037
14. Mejat A, Misteli T (2010) LINC complex in health and disease. Nucleus 1(1):40–52
15. Mattout A, Goldberg M, Tzur Y, Margalit A, Gruenbaum Y (2007) Specific and conserved sequences in *D. melanogaster* and *C. elegans* lamins and histone H2A mediate the attachment of lamins to chromosomes. J Cell Sci 120(Pt 1):77–85. doi:10.1242/jcs.03325
16. Taniura H, Glass C, Gerace L (1995) A chromatin binding site in the tail domain of nuclear lamins that interacts with core histones. J Cell Biol 131(1):33–44
17. Kubben N, Voncken JW, Demmers J, Calis C, van Almen G, Pinto Y, Misteli T (2010) Identification of differential protein interactors of lamin A and progerin. Nucleus 1(6):513–525. doi:10.4161/nucl.1.6.13512
18. Guelen L, Pagie L, Brasset E, Meuleman W, Faza MB, Talhout W, Eussen BH, de Klein A, Wessels L, de Laat W, van Steensel B (2008) Domain organization of human chromosomes revealed by mapping of nuclear lamina interactions. Nature 453(7197):948–951. doi:10.1038/nature06947
19. Polioudaki H, Kourmouli N, Drosou V, Bakou A, Theodoropoulos PA, Singh PB, Giannakouros T, Georgatos SD (2001) Histones H3/H4 form a tight complex with the inner nuclear membrane protein LBR and heterochromatin protein 1. EMBO Rep 2(10):920–925. doi:10.1093/embo-reports/kve199
20. Montes de Oca R, Lee KK, Wilson KL (2005) Binding of barrier to autointegration factor (BAF) to histone H3 and selected linker histones including H1.1. J Biol Chem 280(51):42252–42262. doi:10.1074/jbc.M509917200

21. Antoniacci LM, Kenna MA, Skibbens RV (2007) The nuclear envelope and spindle pole body-associated Mps3 protein bind telomere regulators and function in telomere clustering. Cell Cycle 6(1):75–79
22. Chikashige Y, Tsutsumi C, Yamane M, Okamasa K, Haraguchi T, Hiraoka Y (2006) Meiotic proteins bqt1 and bqt2 tether telomeres to form the bouquet arrangement of chromosomes. Cell 125(1):59–69. doi:10.1016/j.cell.2006.01.048
23. Conrad MN, Lee CY, Wilkerson JL, Dresser ME (2007) MPS3 mediates meiotic bouquet formation in *Saccharomyces cerevisiae*. Proc Natl Acad Sci USA 104(21):8863–8868. doi:10.1073/pnas.0606165104
24. King MC, Drivas TG, Blobel G (2008) A network of nuclear envelope membrane proteins linking centromeres to microtubules. Cell 134(3):427–438. doi:10.1016/j.cell.2008.06.022
25. Gerlitz G, Livnat I, Ziv C, Yarden O, Bustin M, Reiner O (2007) Migration cues induce chromatin alterations. Traffic 8(11):1521–1529. doi:10.1111/j.1600-0854.2007.00638.x
26. Dahl KN, Scaffidi P, Islam MF, Yodh AG, Wilson KL, Misteli T (2006) Distinct structural and mechanical properties of the nuclear lamina in Hutchinson-Gilford progeria syndrome. Proc Natl Acad Sci USA 103(27):10271–10276. doi:10.1073/pnas.0601058103
27. Quintyne NJ, Schroer TA (2002) Distinct cell cycle-dependent roles for dynactin and dynein at centrosomes. J Cell Biol 159(2):245–254. doi:10.1083/jcb.200203089
28. Gonda MA, Aaronson SA, Ellmore N, Zeve VH, Nagashima K (1976) Ultrastructural studies of surface features of human normal and tumor cells in tissue culture by scanning and transmission electron microscopy. J Natl Cancer Inst 56(2):245–263
29. Daigle N, Beaudouin J, Hartnell L, Imreh G, Hallberg E, Lippincott-Schwartz J, Ellenberg J (2001) Nuclear pore complexes form immobile networks and have a very low turnover in live mammalian cells. J Cell Biol 154(1):71–84
30. Andres V, Gonzalez JM (2009) Role of A-type lamins in signaling, transcription, and chromatin organization. J Cell Biol 187(7):945–957. doi:10.1083/jcb.200904124
31. Dittmer TA, Misteli T (2011) The lamin protein family. Genome Biol 12(5):222. doi:10.1186/gb-2011-12-5-222
32. De Sandre-Giovannoli A, Bernard R, Cau P, Navarro C, Amiel J, Boccaccio I, Lyonnet S, Stewart CL, Munnich A, Le Merrer M, Levy N (2003) Lamin a truncation in Hutchinson–Gilford progeria. Science 300(5628):2055. doi:10.1126/science.1084125
33. Eriksson M, Brown WT, Gordon LB, Glynn MW, Singer J, Scott L, Erdos MR, Robbins CM, Moses TY, Berglund P, Dutra A, Pak E, Durkin S, Csoka AB, Boehnke M, Glover TW, Collins FS (2003) Recurrent de novo point mutations in lamin A cause Hutchinson-Gilford progeria syndrome. Nature 423(6937):293–298. doi:10.1038/nature01629
34. Verstraeten VL, Ji JY, Cummings KS, Lee RT, Lammerding J (2008) Increased mechanosensitivity and nuclear stiffness in Hutchinson-Gilford progeria cells: effects of farnesyltransferase inhibitors. Aging Cell 7(3):383–393. doi:10.1111/j.1474-9726.2008.00382.x
35. Hebbar S, Mesngon MT, Guillotte AM, Desai B, Ayala R, Smith DS (2008) Lis1 and Ndel1 influence the timing of nuclear envelope breakdown in neural stem cells. J Cell Biol 182(6):1063–1071. doi:10.1083/jcb.200803071
36. Busson S, Dujardin D, Moreau A, Dompierre J, De Mey JR (1998) Dynein and dynactin are localized to astral microtubules and at cortical sites in mitotic epithelial cells. Curr Biol 8(9):541–544. S0960-9822(98)70208-8 [pii]
37. Schroer TA (2004) Dynactin. Annu Rev Cell Dev Biol 20:759–779. doi:10.1146/annurev.cellbio.20.012103.094623
38. Kardon JR, Vale RD (2009) Regulators of the cytoplasmic dynein motor. Nat Rev Mol Cell Biol 10(12):854–865. doi:10.1038/nrm2804
39. Brandt A, Papagiannouli F, Wagner N, Wilsch-Brauninger M, Braun M, Furlong EE, Loserth S, Wenzl C, Pilot F, Vogt N, Lecuit T, Krohne G, Grosshans J (2006) Developmental control of nuclear size and shape by Kugelkern and Kurzkern. Curr Biol 16(6):543–552. doi:10.1016/j.cub.2006.01.051
40. Hampoelz B, Azou-Gros Y, Fabre R, Markova O, Puech PH, Lecuit T (2011) Microtubule-induced nuclear envelope fluctuations control chromatin dynamics in Drosophila embryos. Development 138(16):3377–3386. doi:10.1242/dev.065706
41. Smetana K, Mikulenkova D, Klamova H (2011) Heterochromatin density (condensation) during cell differentiation and maturation using the human granulocytic lineage of chronic myeloid leukaemia as a convenient model. Folia Biol (Praha) 57(5):216–221. pii: FB2011A0031
42. Bainton DF, Ullyot JL, Farquhar MG (1971) The development of neutrophilic polymorphonuclear leukocytes in human bone marrow. J Exp Med 134(4):907–934
43. Olins AL, Olins DE (2004) Cytoskeletal influences on nuclear shape in granulocytic HL-60 cells. BMC Cell Biol 5:30. doi:10.1186/1471-2121-5-30
44. Olins AL, Ernst A, Zwerger M, Herrmann H, Olins DE (2010) An in vitro model for Pelger-Huet anomaly: stable knockdown of lamin B receptor in HL-60 cells. Nucleus 1(6):506–512. doi:10.4161/nucl.1.6.13271
45. Olins AL, Herrmann H, Lichter P, Kratzmeier M, Doenecke D, Olins DE (2001) Nuclear envelope and chromatin compositional differences comparing undifferentiated and retinoic acid- and phorbol ester-treated HL-60 cells. Exp Cell Res 268(2):115–127. doi:10.1006/excr.2001.5269
46. Crisp M, Liu Q, Roux K, Rattner JB, Shanahan C, Burke B, Stahl PD, Hodzic D (2006) Coupling of the nucleus and cytoplasm: role of the LINC complex. J Cell Biol 172(1):41–53. doi:10.1083/jcb.200509124
47. Haque F, Lloyd DJ, Smallwood DT, Dent CL, Shanahan CM, Fry AM, Trembath RC, Shackleton S (2006) SUN1 interacts with nuclear lamin A and cytoplasmic nesprins to provide a physical connection between the nuclear lamina and the cytoskeleton. Mol Cell Biol 26(10):3738–3751. doi:10.1128/MCB.26.10.3738-3751.2006
48. Haque F, Mazzeo D, Patel JT, Smallwood DT, Ellis JA, Shanahan CM, Shackleton S (2010) Mammalian SUN protein interaction networks at the inner nuclear membrane and their role in laminopathy disease processes. J Biol Chem 285(5):3487–3498. doi:10.1074/jbc.M109.071910
49. Gregory WA, Edmondson JC, Hatten ME, Mason CA (1988) Cytology and neuron-glial apposition of migrating cerebellar granule cells in vitro. J Neurosci 8(5):1728–1738
50. Freitag M, Hickey PC, Raju NB, Selker EU, Read ND (2004) GFP as a tool to analyze the organization, dynamics and function of nuclei and microtubules in *Neurospora crassa*. Fungal Genet Biol 41(10):897–910. doi:10.1016/j.fgb.2004.06.008
51. Ingber DE (2006) Cellular mechanotransduction: putting all the pieces together again. FASEB J 20(7):811–827. doi:10.1096/fj.05-5424rev
52. Wang N, Tytell JD, Ingber DE (2009) Mechanotransduction at a distance: mechanically coupling the extracellular matrix with the nucleus. Nat Rev Mol Cell Biol 10(1):75–82. doi:10.1038/nrm2594